

*“We cannot solve our problems with the  
same thinking we used when we created  
them”*

*Albert Einstein*

## **Chapter 3. 3D Lung Pathology Imaging**

**Abstract:** Three dimensional, structural and functional digital image databases have many applications in education, research and clinical medicine. To date, with the exception of cryosectioning, there have been no reliable means to obtain whole-organ, spatially conserving histology. Our aim was to generate a system capable of acquiring high-resolution lung pathology images featuring microscopic detail that could still be spatially correlated to whole organ non-invasive imaging systems such as Computed Tomography. To fulfill these objectives required the construction of a system physically capable of creating very fine whole organ sections and collecting high-magnification and resolution digital images. We therefore designed a large image microscope array (LIMA) to serially section and image entire un-embedded lung specimens while maintaining the structural integrity of the tissue. The LIMA consists of several integrated components including: a novel large-blade vibrating microtome, a 1.3 megapixel peltier cooled CCD camera, a high magnification microscope and a three-axis gantry above the microtome. A custom control software program was developed to automate the entire sectioning and raster-scan imaging sequence. The system is capable of sectioning un-embedded soft tissue down to a thickness of 40  $\mu\text{m}$  at specimen dimensions of 200 mm by 300 mm to a total depth of 350 mm.

In the following chapter, we demonstrate the ability of the LIMA system through a series of tests using fixed lung from sheep and mice, resulting in large high quality image datasets with minimal distinguishable disturbance in the delicate alveolar structures.

### **3.1 Introduction**

The combination of both destructive and non-destructive imaging modalities when spatially registered, can provide a useful map of anatomical structure with the potential to provide functional insight. Undertakings such as the Visible Human

Project have created a multi-modal, three-dimensional representation of a male and a female cadaver [132]. The primary modalities include computed tomography (CT), magnetic resonance imaging (MRI) and cryosectioned digital pathology images. These datasets were created as a common reference point for the study of human gross anatomy and have been applied in diagnosis, education, virtual reality, and industry [133]. The Visible Human Project cryosections feature one digital image per slice of tissue, such that the resolution of the digital pathology images is comparable to that of the other imaging modalities. When studying gross anatomy, this resolution provides an acceptable degree of detail. In situations where fine structural details and more specific histology are needed, higher resolution images are required.

Visual investigation of specific organ tissue in normal and diseased states is commonly performed using some form of histology. Traditional histology and pathology techniques introduce destructive and spatial artifacts. Advancements in microscopy that incorporate some automation in the collection and analysis of pathology images have recently been made. The commercially available Ariol SL-50 (Applied Imaging, San Jose) is one example of an automated system incorporating microscopy, digital image acquisition, archiving, and image processing for microscope slides. A more complete automated system, developed by Fernandez-Gonzalez et al. [134], provides a means for three-dimensional morphological and molecular analysis of thick tissue specimens, through sequential high-resolution acquisition of histology slides prepared serially through a large specimen, such as a whole gland. Their approach has been successful for histology slides, but inherently requires semi-automated registration between slices due to the shrinkage artifacts caused through preparation of the slides.

The most significant restrictions in histology, in both manual and automated techniques for representing whole organ pathology, are two fold. First, the pathology sections are small in relation to the spatial volume of the organ. Second, the discrete pathology samples are two dimensional with little volumetric spatial correspondence. This means that direct comparison of the microscopic structure to three dimensional imaging modalities is difficult and tedious at best. Clearly a need exists to improve current techniques for evaluation of organ structure between large-

scale macroscopic sections to small-scale microscopic histology. Such spatial correspondence is of paramount importance and must be maintained for accurate correlation to be successful across different three-dimensional modalities.

Our aim was to generate a system capable of acquiring high-resolution images featuring microscopic detail that could still be spatially correlated to the whole organ. The fulfillment of these objectives required the construction of a system physically capable of creating very fine whole organ sections and collecting high-magnification and resolution digital images. The system magnification had to be variable in order to reach the desired level of microscopic structure in an organ while minimizing the size of the datasets to image a large-scale organ volume. We chose the lung as our organ of interest, which created several challenges - the lung is not a solid organ and its structure is delicate and hard to maintain using standard histology fixation, both through chemical or cryo-techniques.

## **3.2 Methods**

### **3.2.1 Microtome Development**

Due to the lack of an appropriate sectioning instrument for large un-embedded soft tissue in the commercial market, a Leica SM2500M manual microtome was purchased and modified as shown in Figure 3.1. The original microtome was designed for large-scale, heavy-duty sectioning of specimens embedded in paraffin or resin. Movement of the stage was completely manual, controlled via a hand crank assembly. The stage moves towards the fixed knife assembly and is retracted after each section. The knife assembly was re-designed to house a custom built large-scale vibrating blade in order to smoothly section soft tissue without the need for tissue embedment. This path was taken since tissue processing for embedding, in particular paraffin causes many of the artifacts seen in lung histology. Embedding with resins is not an option for such a large volume due to heat build up during polymerization. In addition, to maintain vertical alignment between sections, images would be acquired en-bloc (from the surface of the remaining tissue). Precise control over the microtome tissue stage position was then necessary to ensure alignment between subsequent sections.

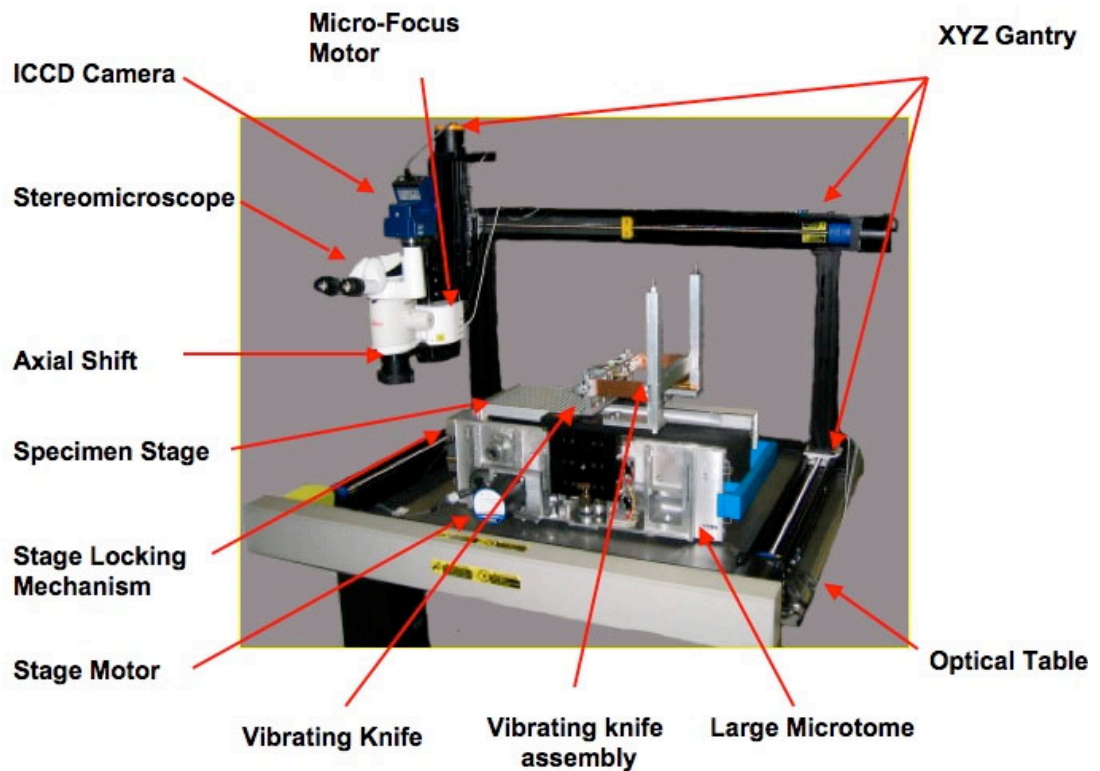


Figure 3.1: The large image microscope array (LIMA) system shown with; a CCD digital camera mounted to a stereomicroscope, which are both positioned over the specimen stage via a gantry to image the tissue en bloc.

### 3.2.2 Microtome Motorization

We motorized the tissue stage so that a uniform cutting speed could be maintained through the sectioning process to facilitate greater repeatability and reliability. By replacing the manual control with electronic control, the tissue stage was also interfaced with a computer for automation. A 200 step per revolution Slo-Syn (Superior Electric, Connecticut) stepper motor and 6:1 gear system were integrated to control the tissue stage through the sectioning process. Since image acquisition was performed off the cut-tissue block and the maintenance of alignment in the z-axis was paramount, a high precision stopping mechanism with micron accuracy was also introduced.

### 3.2.3 Vibrating Blade Microtome Development

Extensive experimentation was conducted to develop an optimal vibrating knife system, for sectioning non-embedded tissue. While high frequency motion was effective in cutting through the majority of tissues, some difficulty was experienced in simultaneously sectioning the delicate lung structure and dense airway walls. Hence the vibrating blade was designed to vibrate at both a *high* frequency and a *low* frequency. Figure 3.2 represents a schematic of the vibrating knife assembly. Leaf springs connect the base bracket to the vibration frame, allowing horizontal motion while restricting vibration vertically. The vibration frame holds an air pressure-driven linear vibrator, which produces a high frequency variable linear oscillation via a piston and back trap manifold. Mounted on the base bracket is also a gear motor and spring assembly, which provides very-low-frequency motion to the vibration frame through a horizontally configured rod and spring system as shown in Figure 3.2. The high frequency motion can be set by the user within a range of 80 to 110 Hz. When sectioning soft, spongy structures such as lung tissue, the secondary much lower frequency vibration provides a saw-like oscillation to aid the blade's procession through the tissue. There are two separate systems for controlling the amplitudes and frequencies of the vibrating knife. High frequency control is achieved through the relationships between applied air pressure and the oscillation frequency of the linear vibrator. Low frequency vibration is controlled via the voltage applied to the gear motor. The knife itself is a 26 cm surgical trimming blade held via a custom vice mechanism in the vibration frame. Using this system, sections are removed and can be saved for further histology.

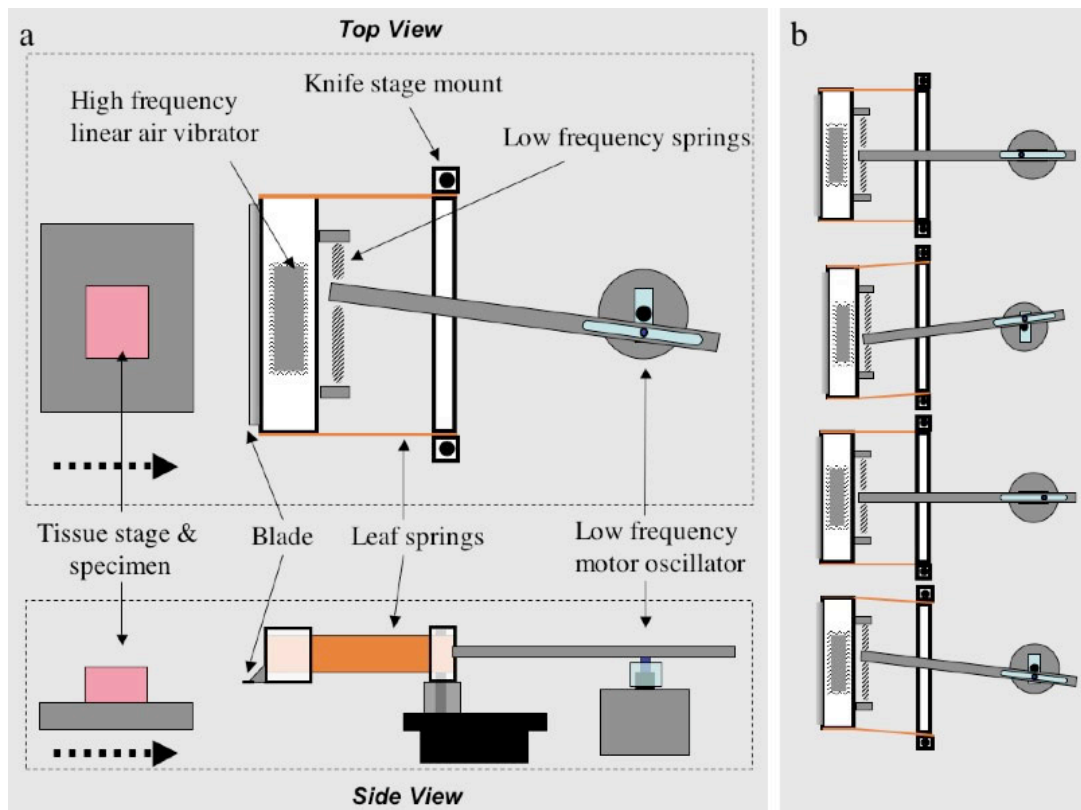


Figure 3.2: (a) represents a schematic of the large-scale dual-frequency vibrating knife system from a top and side view. (b) a pictorial representation of the low frequency motion through rotation of the motor assembly and high frequency motion as depicted by the waves protruding from the linear air vibrator.

### 3.2.4 Photo Lock

A "photo locking" mechanism was designed to ensure the microtome stage returns to the same location between sections. The motorized stage returns to the "photo lock" position via the computer controlled stepper motor. Once in the "photo lock" position, a mechanism consisting of a tapered rod is pushed via a solenoid into a matching tapered hole and achieves the final locking of the stage. This locking mechanism can be seen on the left hand side of the microtome in Figure 3.3 (a) with the locking sequence shown in greater detail in Figure 3.3 (b). The solenoid is normally locked and energy is applied to the solenoid to unlock during sectioning. This ensures the solenoid is off during imaging and does not add unnecessary vibration to the system.

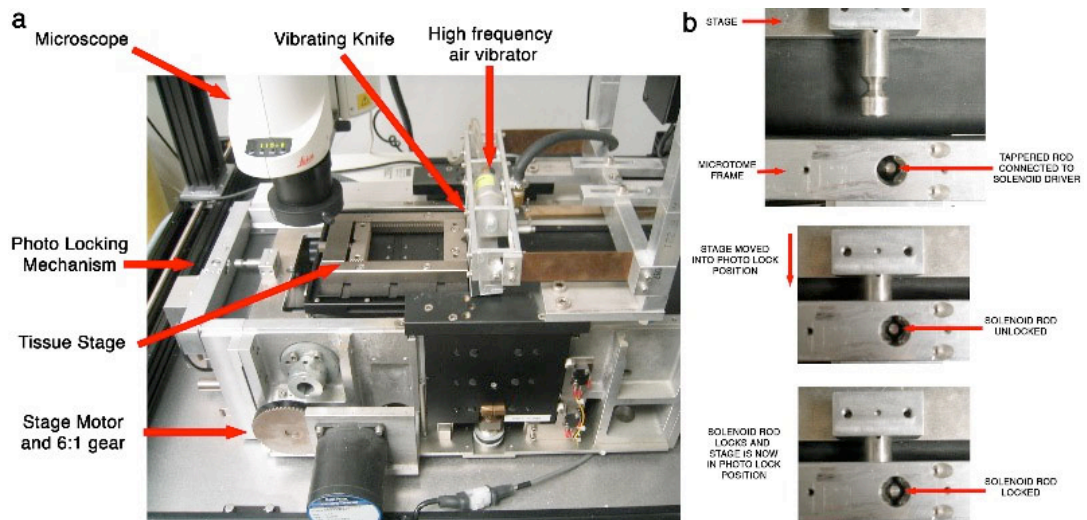


Figure 3.3: (a) shows the microtome and locking mechanism (on the left) that ensures correct positioning of the stage for image acquisition. (b) shows a close up of the “photo locking” mechanism prior to an imaging sequence.

### 3.2.5 Imaging System

The imaging system is composed of a Leica MZ16FA (Leica Microsystems GmbH, Germany) stereomicroscope configured with a 1x plan achromatic objective and a JenOptik C14 (Jenoptik GmbH, Germany) cooled scientific camera. This specific microscope carrier and camera couple was selected for its flexibility in performing bright field and dark field fluorescent microscopy of stained and non-stained specimens. To remove the "stereo" angle and create a perpendicular line of sight for the acquired images, a Leica axial shift adapter was mounted between the objective and the stereoscope. The microscope has a magnification range of 7.11x to 115x with a maximum resolution of 420 line pairs in this configuration. Digital images are acquired through the JenOptik C12 cooled charge-coupled device (CCD) digital camera. The peltier cooling reduces the dark currents, which allows for dark field fluorescent imaging. The CCD contains a 1300x1030 pixel array with a pixel pitch of 6.7  $\mu\text{m}$ . The camera has a multi-shot feature that can be used to increase the effective pixel count from 1.3 megapixels to 12 megapixels. Image data acquired by the camera is transferred via a Firewire IEEE 1394 interface to the computer.

During image acquisition, the vibratome stage is locked into the “photo lock” location and the blade vibration is stopped. The LIMA system is also positioned on a Micro-g (TMC, Massachusetts) vibration isolation optical table to minimize

environmental vibrations, as image acquisition particularly in multi-shot mode is highly sensitive. The microscope and CCD camera coupling is maneuvered above the sectioned tissue surface via a Velmex Bislide (Velmex, New York) parallel-coupled gantry system. The gantry consists of 94 cm parallel bislides in the y axis, a 112 cm single bislide in the x axis, and a 25 cm single bislide in the z axis. Control of the gantry motion is automated via three computer-interfaced stepper motors. A standard PC is used for both computer automation and image acquisition.

### **3.2.6 Automation Software**

A high level of precision is needed in sectioning tissue samples and positioning the microscope and camera couple. This precision requirement, when coupled with the highly repetitive and time-consuming nature of multiple, sequential image acquisition, necessitates system automation. Microsoft's .NET framework, specifically Managed C++, was chosen as the programming language to design the controller for the automation of the LIMA hardware and to provide an efficient graphical user interface, as seen in Figure 3.4.

The automation program for the LIMA system consists of controls for the three major tasks involved: initialization, sectioning and imaging. The initialization stage sets up the serial port connections between the computer and the stepper motors of the gantry and microtome as well as provides output paths for image storage and name formatting. The microtome control provides the user with the ability to position the tissue stage in the most convenient position for specimen attachment. Activation of the low and high frequency oscillations is also automated. A grossing option is included to section the tissue down to the level where image acquisition is to be initiated. The user is able to select the top left and bottom right edges of the specimen using the gantry controls on the program while visual feedback is provided from the image seen through the CCD camera onto the computer screen. When each corner is selected, the program computes the correct raster scan image acquisition sequence using the current field of view and magnification settings, which are also set via the computer program. Once the microscope is focused on the specimen for the first slice, the software automatically detects the best focus position for all subsequent slices by maximizing the high frequency components of

the acquired images. As scanning commences, the images are overlapped onto the screen as they are acquired to form the entire image.

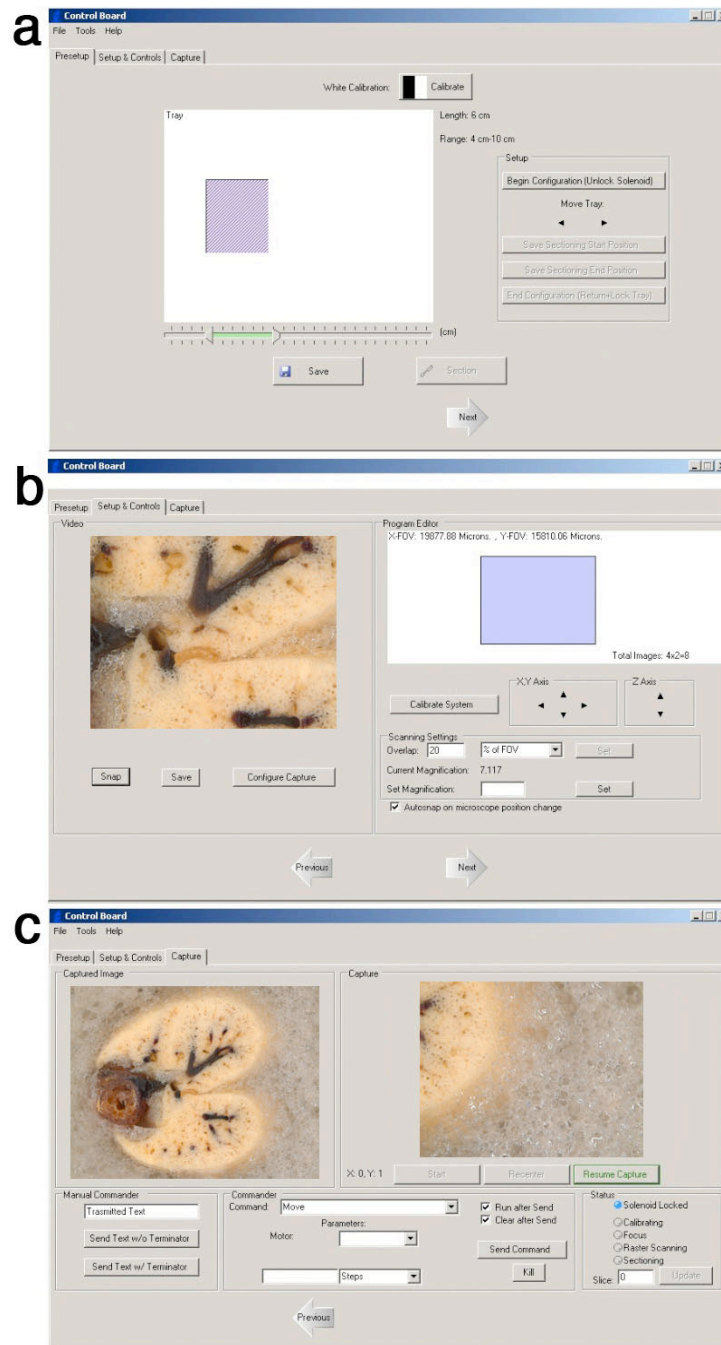
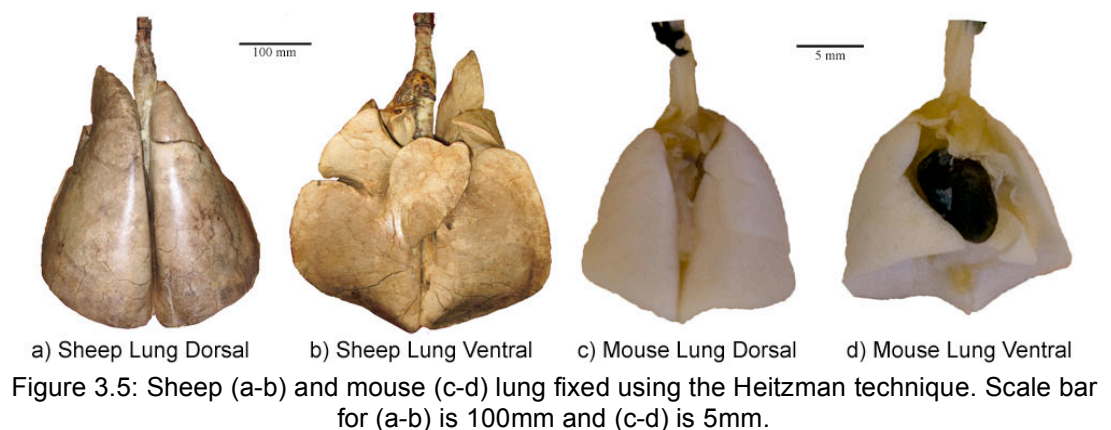


Figure 3.4: The graphical user interface used to control the functions of the LIMA system. (a) the tissue setup phase, where the user interactively selects the area of the microtome stage that includes the tissue specimen. (b) the image preparation step, where the user interactively determines the centre of the tissue specimen, along with the magnification, field of view and boundaries for image acquisition. (c) left panel shows the current high magnification image which is being captured and the right panel shows the completed montage of the sub-images.

### 3.2.7 Lung Tissue Preparation

Lung tissue which is sectioned and imaged on the LIMA system is fixed using a modified Heitzman method [31]. This fixation technique conserves radio-density while maintaining necessary histopathology for accurate pathologic and radiologic comparisons. In brief, the lungs are fixed and inflated with a fixation mixture consisting of 25% Polyethylene Glycol 400 (FisherChemicals, New Jersey), 10% Ethyl Alcohol (190 Proof, 95%) (Pharmco Products, Connecticut), 10% Formaldehyde Solution (FisherChemicals, New Jersey) and 55% laboratory distilled water. The fixation fluid is applied intra-tracheally at 15cm water pressure through a gravity feed system for 12 hours for mice or 48 hours for whole sheep lung while immersed in the fixation mixture. Intra-tracheal administration allows the fixation fluid to reach within a short space of all the tissue, since the airways essentially fill the lung in a fractal manner. Also placing the lung in the fixative ensures that areas inaccessible via the airways are fixed through diffusion. The lung is then disconnected from the fixation apparatus and air-dried at 15 cm water pressure for several days in a heated drying oven set to 60 degrees Celsius. Using this method there is minimal reduction in lung volume during fixation; and the lung density as measured by the CT scan before and after fixation, is preserved.

Examples of lungs, fixed using the described Heitzman technique, from both a sheep and a mouse are shown in Figure 3.5.



### 3.2.8 Mouse Lung Agarose Embedding

Mice lungs are externally embedded using agarose to ensure the lung tissue is well supported during sectioning. The agarose is made from standard biological grade agarose, mixed with distilled water and heated in a microwave on high for 20 seconds. The agarose is allowed to cool down to 10 degrees above the gelling temperature and then poured into a custom container which houses the mouse lung in the correct orientation with respect to the *ex vivo* micro-CT scan [135]. The container is then placed in a refrigerator where the agarose is allowed to gel and cool for an additional 6 hours.

### 3.2.9 Solid Tissue Preparation

Solid tissue specimens can also be used on the LIMA system and, depending on the organ of interest, may not require fixation. One example is brain tissue which, with the correct temperature control and nutrient availability, could be sectioned and imaged live as performed on standard vibratome systems.

In other cases, the tissue could be fixed using vascular perfusion techniques to ensure the fixative (not confined to the Heitzmen technique, and could be formalin) permeates through the entire organ of interest. Such organs could then be externally embedded into a container using the agarose mixture outlined for mouse lungs.

### 3.2.10 Standard Histology and Immunohistochemical Staining

Tissue sectioned and imaged on the LIMA system can then be stored in PBS solution and processed for standard Hematoxylin and Eosin (H&E) histology as well as immunohistochemistry. For immunohistochemistry, a shorter interval between fixation, sectioning and slide preparation produces better final results.

### 3.2.11 Image Acquisition

By imaging the surface of the tissue en-bloc, the spatial relationships between each sequential slice can be maintained. The microscope and the camera are moved

through an automated raster scan in order to capture the entire surface area of the tissue via multiple high magnification images. A registration algorithm was created to register the overlapping portions of the sub-images to create a reliably aligned composite image of the complete tissue surface [136]. This differs from traditional pathology where imaging is performed on distinct tissue sections mounted on microscope slides.

Due to the large number of images required to complete a whole-organ image dataset, storage is a pertinent consideration. The average dimension of a sheep or human lung can be estimated at 20 cm by 10 cm in the transverse plane. To section at 250  $\mu\text{m}$  for a depth of 1 cm and acquire images at the highest system magnification of 115x, roughly 700,000 images would be required. This would require approximately 1.2 terabytes of storage for the entire dataset if an uncompressed portable network graphics (png) file format were used. A balance between the resolution, magnification, slice thickness and image compression must be made for each project in order to increase the useful information, without storing redundant information.

In our standard whole mouse lung imaging, we acquire 50 images (40x magnification) per slice for 70 slices (250 micron thick slices), generating 3,500 images. These are saved in a loss-less TIFF format requiring 1 megabyte per image. The resultant data set of 3-4 gigabytes is now a manageable size for storage, processing and analysis.

### 3.3 Results

#### 3.3.1 Fixed Sheep Lung Specimens

Fixed, inflated lung specimens from sheep using the modified Heitzmen technique as outlines in the methods have been examined. The upper left lobe of a sheep lung was removed and scanned on a clinical computed tomography (CT) scanner (Siemens Sensation 16, Germany). The lobe was then mounted onto the tissue stage of the LIMA microtome using a custom container and agarose external embedding, similar to the system used for mouse lungs. The lobe was sectioned at 250-micron slice thickness and imaged using the LIMA system. With a magnification of 20x, 84 images were required to capture the entire lobe section per slice. Images for each LIMA slice were stitched into a single composite image as shown in Figure 3.6 (b) and slices from the LIMA data set were then aligned with their corresponding CT slice as shown in Figure 3.6 (a).

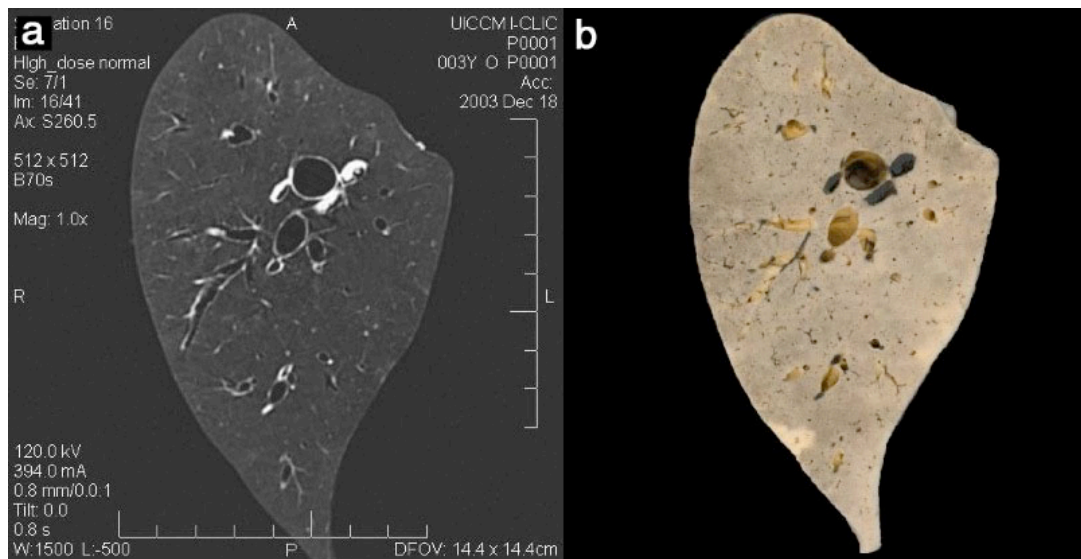


Figure 3.6: (a) represents a CT slice from the upper lobe of a fixed sheep lung and figure 5 (b) represents the corresponding stitched LIMA image.

Small sections (20x20mm) of fixed sheep lung have also been imaged using a combination of micro-CT, LIMA and histopathology in order to compliment the information provided by each technique: radio-density information in micro-CT, color/fluorescent marker information in LIMA, and cellular content in the histopathology. Figure 3.7 illustrates a slice of tissue as represented following

registration, from the LIMA, micro-CT and H&E histology imaging modalities [137].

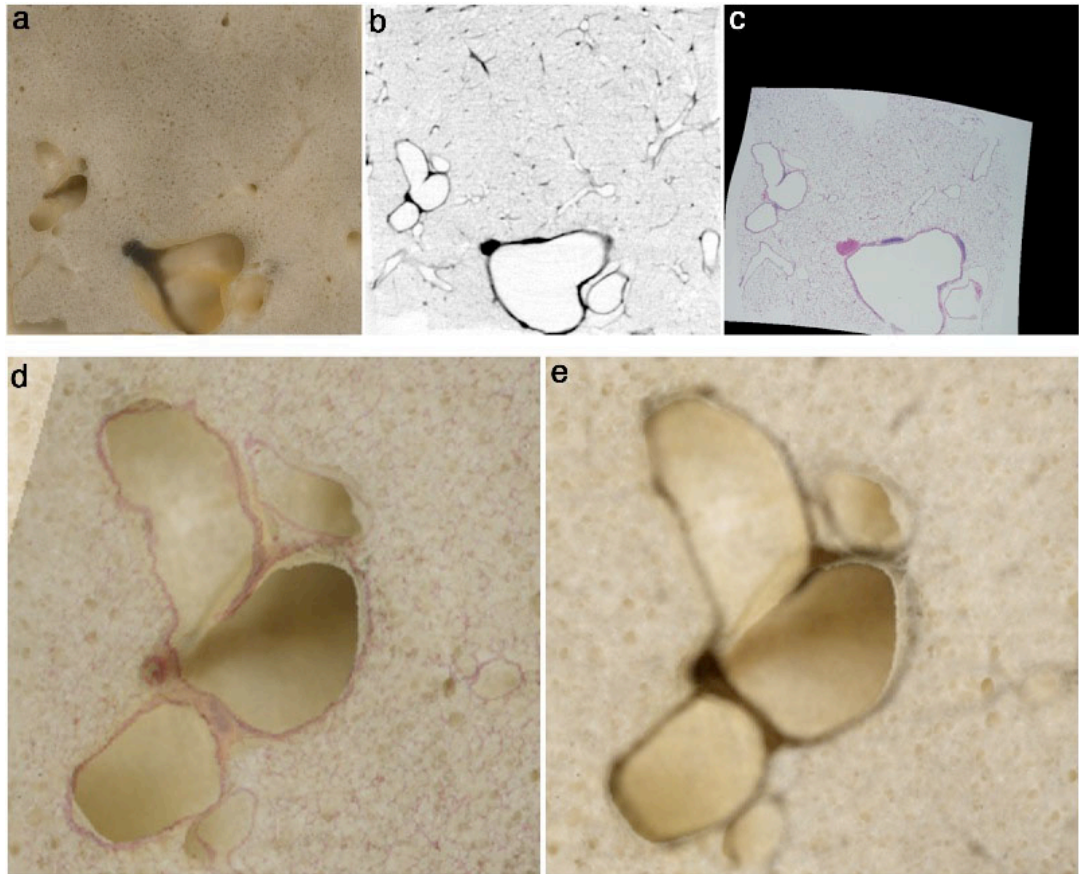


Figure 3.7: An example application of the LIMA system for the registration of a multi-modal fixed sheep lung dataset. (a) represents the color LIMA image, (b) represents the micro-CT radiological image and finally (c) represents the H&E histopathology image, from the same location. The images have been registered using a thin-plate spline algorithm and the final multi-modal dataset provides registered radio-density, color and cellular information. In (d) and (e), a small area to the left of images (a-b) has been magnified to reveal the strong correlation between the registered H&E histology and micro-CT image with respect to the LIMA dataset.

### 3.3.2 Fixed Mouse Lung Specimens

In addition to large animal specimens, the LIMA system is used to visualize small animal organs. The entire normal mouse lung has been sectioned and imaged using the LIMA system. An *in vivo* micro-CT data set is initially acquired using the Intermittent Iso-pressure Breath Hold (IIBH) technique [138], as detailed in Section 4.3. The lung is excised and fixed, as detailed in the methods, and scanned on the micro-CT scanner using a custom made container shown in Figure 3.8, which

maintains orientation between the micro-CT imaging and the following LIMA cross sectioning and imaging.

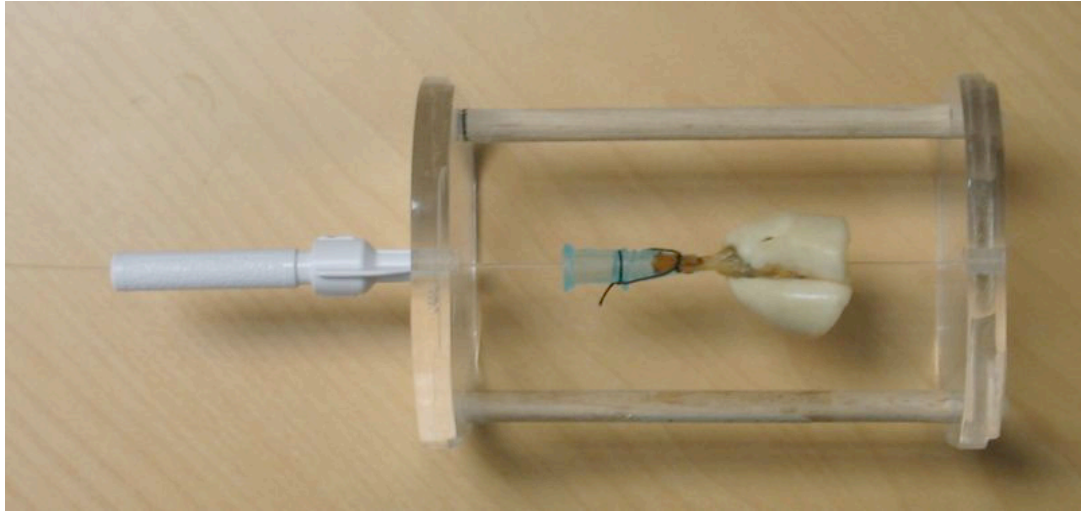


Figure 3.8: Mouse lung mounted inside the Micro-CT and LIMA static orientation device.

The excised lung in its fixed orientation container is agarose embedded and serially sectioned and imaged on the LIMA system. Each tissue section removed from the LIMA system is then stored in PBS solution and processed for histopathology. This entire image acquisition and registration process is illustrated in Figure 3.9. An example of an axial slice registered from the *in vivo* micro-CT, fixed lung micro-CT, stitched LIMA and high-resolution H&E image is shown in Figure 3.10 (a-d), respectively.

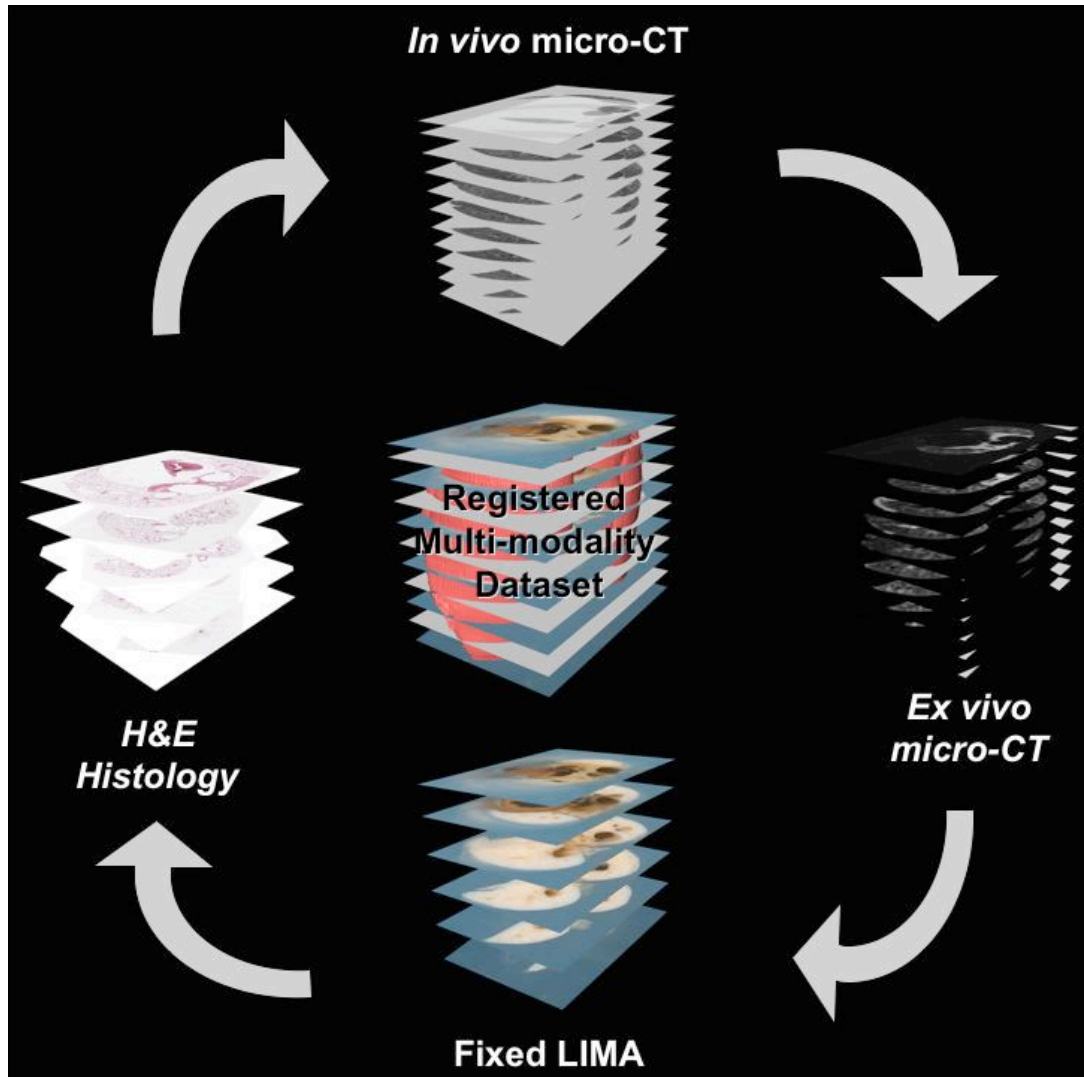


Figure 3.9: Image acquisition and registration pipeline using the *ex vivo* micro-CT and LIMA datasets as the reference.

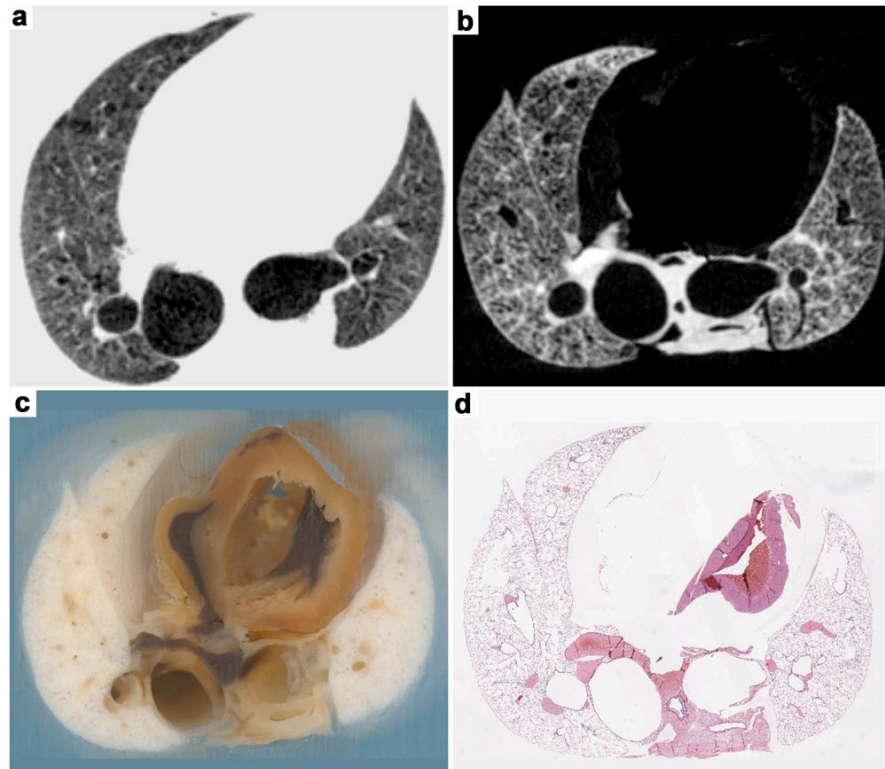


Figure 3.10: An example of a registered mouse lung dataset from the *in vivo* state down to the histology level can be seen. (a) represents a 28-micron slice from the original *in vivo* micro-computed tomography scan. (b) represents a 28-micron slice from the fixed *ex vivo* micro-computed tomography scan. (c) represents a final LIMA image, stitched from 49 sub-images at 40x magnification. Finally, (d) represents the corresponding H&E histopathology image for the same slice. In this example we can see the advantage of the LIMA system in providing spatial correlation between a non-destructive three-dimensional modality such as the micro-CT with respect to the destructive histopathology imaging.

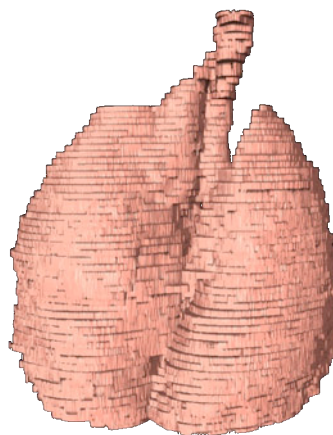


Figure 3.11: 3D representation of the entire mouse lung boundary obtained from the LIMA system is shown; clearly the non iso-tropic nature of this imaging system is evident by the jarred edges between slices.

### **3.4 Discussion**

Modification of the Leica SM2500 microtome into a large scale vibrating microtome with both low- and high-frequency oscillation was successful in achieving whole fixed, non-embedded organ sections. A custom x-y-z gantry system was successfully developed to move the microscope and CCD camera over the entire sectioned tissue surface for acquisition of high magnification images of the organ surface while maintaining spatial integrity with respect to the organ volume. Acquiring images en-bloc, rather than the resultant thin sliced sections (as performed in standard histology), minimized distortion of the tissue structure and maintained alignment of subsequent sections.

Large and small animal lung specimens were selected for testing the LIMA. Some organs such as the normal brain are reasonably solid and have a consistent texture throughout the organ, whereas lung tissue is non-solid and contains varying tissue characteristics with important fine structural features. The conducting airway walls are relatively thick and tough, while the walls of the terminal alveolar sacs are extremely thin and fragile. The dual vibration frequency of the vibrating microtome enables the sectioning of the lung tissue with very minimal visible disturbance to the underlying alveolar structures.

The LIMA system is being utilized for a number of investigations in pulmonary imaging, bridging the gap between non-destructive imaging techniques such as CT and MRI and destructive techniques such as histology. Validation of automated segmentation algorithms for airways and vessels based on CT datasets can be performed using registered CT and LIMA data sets, such as those shown in Figure 3.6 (a) and Figure 3.6 (b). Here, correlation of the anatomic truth with the representative CT image can be accurately performed with greater confidence. In Figure 3.7 (a)-(c), the LIMA slice has been accurately registered to the representative micro-CT and histology slice. In Figure 3.7 (d) & (e), a high magnification image of the histology overlaid onto the LIMA image and the micro-CT image overlaid onto the LIMA image is shown, respectively. As seen in this example accurate registration between the three-modalities can be performed. This allows for accurate correlation between the micro-CT and histology data from which

automated pattern classification systems for evaluating the tissue's structural detail directly from the micro-CT data can be developed with much greater precision. This application can be extended to *in vivo* registration where data from an *in vivo* clinical CT can be accurately registered to histology and immunohistopathology. This registration allows “ground truth” validation of the tissue of interest as seen in the CT images, based on accurate knowledge of the cellular state acquired through the registered histology images.

An application currently under investigation is the characterization of human lung cancer nodules as seen *in vivo* from a clinical CT image. The nodules are resected and imaged on a micro-CT followed by the LIMA system to provide information about their cellular content. Early results indicated that ‘malignant’ lung nodules contain heterogeneous structure with varying proportions of cancer tumor cells, necrotic tumor cells fibroblastic tissue and inflammation. Understanding this structure in 3D is very important for tumor biology and for assessing tumor growth and response to therapy. This investigation also provides important information about the ability to identify malignant nodules using standard biopsy techniques, and upcoming micro-optical biopsy procedures [139, 140].

A second application, described in Chapter 6, is characterization of lung nodules in mice. *In vivo* micro-CT images are being acquired from normal mice induced with cancer through administration of Urethane, a carcinogenic agent. Micro-CT images are acquired over a six-month period; finally, the mouse is euthanized and the lungs are fixed and imaged on the LIMA, followed by histology. Initial results indicate the ability to evaluate nodule size, number and growth rates regionally on individual mice and assess pathology content as seen through the registered LIMA and histology data. Only through a system like the LIMA could we accurately analyze individual nodule histology in 3D and correlate back to the 3D micro-CT radio-density information.

The LIMA system has also been used to acquire the first 3D pathology representations of the entire mouse at 250  $\mu\text{m}$  slice increments [135]. The 3D reconstruction of the LIMA stacks in Figure 3.11 have jarred edges between slices, which is due to the non-isotropic nature of the voxels, specifically, higher resolution

in the x and y axes as compared to the z axis. This effect can be reduced through thinner sections as well as the incorporation of interpolation algorithms. Using the LIMA, we can now accurately translate the true *in vivo* reference lung volume as determined using the micro-CT and histology via the LIMA dataset. This is performed by measuring the change in lung volume from the *in vivo* micro-CT lung volume, to the *ex vivo* fixed micro-CT lung volume, to the LIMA lung volume and finally to the histology lung volume. This allows greater repeatability and accuracy in morphometric calculations made at the histology level, a problem that is always of concern in lung stereology [141, 142].

### **3.5 Conclusion**

We have developed a flexible, large-image microscope array system to section un-embedded whole organs and gain high magnification digital images of each cut surface. Custom control software has been successfully developed to automate the entire process of sectioning and image acquisition, creating an efficient system for whole organ 3D pathology acquisition. Finally, we have described and illustrated several multi-modal imaging applications utilizing this system.

